Amplitude analysis of the $\overline{NN}\to\pi^-\pi^+$ reaction

W. M. Kloet
Department of Physics and Astronomy, Rutgers University, Piscataway, New Jersey 08855

F. Myhrer
Department of Physics and Astronomy, University of South Carolina, Columbia, South Carolina 29208
and NORDITA, Blegdamsvej 17, DK-2100 Copenhagen Ø, Denmark

(Received 26 October 1995)

A simple partial wave amplitude analysis of $\overline{pp}\to\pi^-\pi^+$ has been performed for data in the range $p_{\rm lab}$= 360–1000 MeV/c, where remarkably few partial waves are required to fit the data. Furthermore, the number of required J values does not change in this energy range. However, the resulting set of partial wave amplitudes is not unique. We discuss possible measurements with polarized beam and target which will severely restrict and help resolve the present analysis ambiguities. New data from the reaction $\overline{pp}\to\pi^0\pi^0$ alone are insufficient for that purpose. [S0556-2821(96)03411-X]

PACS number(s): 13.75.Cs, 13.75.Gx, 13.88.+e, 25.43.+t

I. INTRODUCTION

Although the reactions $\overline{NN}\to\pi^-\pi^+$ and $\overline{NN}\to K^-K^+$ only account for less than one percent of the $\overline{NN}$ total annihilation cross section, they are two of the more basic annihilation and subsequent hadronization reactions. Therefore, a careful study of these reactions can reveal details of the underlying mechanisms and may clarify the nature of the degrees of freedom necessary to describe these short range hadronic processes. The new low energy data for $\overline{pp}\to\pi^-\pi^+$ (and $\overline{pp}\to K^-K^+$) from the CERN Low Energy Antiproton Ring (LEAR) [1] complement and extend the earlier data [2–4] and show a rather rich energy and spin dependence. The data below $p_{\rm lab}$ = 1.3 GeV/c show considerable angular structure at each energy for both the differential cross section and the analyzing power. In addition, there is considerable change in the angular dependence of the observables with increasing energy at these lower energies. This is in contrast with the region above $p_{\rm lab}$ = 1.3 GeV/c where there is considerably less energy dependence in the angular structure of these two observables. Several analyses of the data of this reaction have been performed [5–9] with the pre-LEAR data. In this paper we will concentrate on the reaction $\overline{pp}\to\pi^-\pi^+$.

The recently published LEAR data were included in the newest Durham analysis [10] which, like the older analyses, writes the two amplitudes (nonspinflip and spinflip) as one analytic function of $w=e^{i\theta}$ where θ is the scattering angle. This function is then parametrized by a *finite* number of Barrelet zeros in the complex w plane. The Barrelet zeros *close* to the physical region show up as local minima in the angular dependence of the spin-dependent cross sections. The invariant mass region of their analysis covers 1910–2273 MeV, and they require 8–10 complex zeros to fit the data at a given energy. The energy dependence of the resulting parametrization shows a rich resonance structure in several partial waves.

The most recent analysis of this reaction by Hasan and Bugg [11] starts from the ansatz that each partial wave amplitude of given L and J is a sum of up to four resonances (of the same J) of different masses and widths. The maximum J value is J = 5, so there are roughly one hundred parameters in their fit. The resonance parameters are then fitted simultaneously to all available data in the energy region of 1930–2530 MeV. Because of the above ansatz, the resulting partial wave amplitudes exhibit counterclockwise motion in the Argand plots. However, they find only clear peaks for the J = 4 and 5 amplitudes. In Ref. [11] it is stated that the observables are approximately symmetric about cos θ = 0. As we see it, this statement does not reflect the data. For example, the $d\sigma/d\Omega$ is forward peaked at low energy ($p_{\rm lab}$ = 360 MeV/c) and backward peaked at energies above $p_{\rm lab}$ = 800 MeV/c and no symmetry about cos θ = 0 is apparent.

II. ANALYSIS

In this paper we report on a different but very simple amplitude analysis of the same data but we restrict our analysis to the momentum range $p_{\rm lab}$ = 360–988 MeV/c, the lowest measured momenta. This $p_{\rm lab}$ range corresponds to an invariant mass region of 1910–2078 MeV. As we will show, in this energy range the number of required partial waves does not change. Since the existing annihilation models do not give a consistent dynamical behavior for the amplitudes, we reduce the theoretical input of this analysis to a minimum. Our main working hypothesis will be that very few partial waves contribute to this particular annihilation reaction. This hypothesis is based on the experience gained by reproducing the observables of this reaction with a simple black sphere model at higher energies ($p_{\rm lab}$>1 GeV/c) [12]. In terms of the two independent helicity amplitudes f_{++} and f_{+-} for this annihilation reaction, the two measured observables are the differential cross section

$$d\sigma/d\Omega=(|f_{++}|^2+|f_{+-}|^2)/2, \tag{1}$$

and the analyzing power A_{on}, defined by

$$A_{on}d\sigma/d\Omega=\mathrm{Im}(f_{++}f_{+-}^{*}). \tag{2}$$

We use here the convention that $\hat{\mathbf{n}}$ is the spin direction normal to the scattering plane. The unit-vector $\hat{\mathbf{n}}$ is along $\vec{p}\times\vec{q}$, where $\vec{p}$ is the antiproton center-of-mass (c.m.) momentum and $\vec{q}$ is the c.m. momentum of π^-. There are additional spin observables. We define the longitudinal spin direction $\hat{\boldsymbol{l}}$ along $\vec{p}$, and the transverse spin direction $\hat{\mathbf{s}}$ is defined to be along $\hat{\mathbf{n}}\times\hat{\boldsymbol{l}}$. The analyzing powers A_{ol} and A_{os} both vanish because of parity conservation. Some spin-correlation observables A_{ij}, for this reaction are, however, nonzero. Of these observables $A_{nn}=1$, but A_{ll}, A_{ss}, A_{sl}, and A_{ls} are nontrivial, with the identities $A_{sl}=A_{ls}$ and $A_{ss}=-A_{ll}$. The observables A_{ss} and A_{ls} can be expressed in the helicity amplitudes respectively, by,

$$A_{ss}d\sigma/d\Omega=(|f_{++}|^2-|f_{+-}|^2)/2, \tag{3}$$

and

$$A_{ls}d\sigma/d\Omega=\mathrm{Re}(f_{++}f_{+-}^{*}). \tag{4}$$

Unfortunately, no data on spin correlations is as yet available. As we shall discuss later, it is necessary to measure at least a third observable of the reaction $\overline{pp}\to\pi^-\pi^+$ (and $p\,\overline{p}\to K^-K^+$) to restrict further the amplitude analysis. From the above four equations one can show that the four observables are related by

$$A_{on}^2+A_{ss}^2+A_{ls}^2=1. \tag{5}$$

The two helicity amplitudes are expanded in $J\neq L$ spin-triplet partial wave amplitudes:

$$f_{++}=\frac{1}{p}\sum_J\ \sqrt{J+\frac{1}{2}}(\sqrt{J}f_{J-1}^J-\sqrt{J+1}f_{J+1}^J)P_J(\cos\theta) \tag{6}$$

and

$$f_{+-}=\frac{1}{p}\sum_J\ \sqrt{J+\frac{1}{2}}\left(\frac{1}{\sqrt{J}}f_{J-1}^J+\frac{1}{\sqrt{J+1}}f_{J+1}^J\right)\times P_J'(\cos\theta)\sin\theta, \tag{7}$$

where P_J' denotes the first derivative of the Legendre polynomial P_J.

In our analysis of the existing data of $\overline{pp}\to\pi^-\pi^+$, we parametrize the partial wave amplitudes at each energy as

$$f_L^J=R_{LJ}e^{i\delta_{LJ}}, \tag{8}$$

where R_{LJ} and δ_{LJ} are our free parameters. At each energy we choose the maximum J to be included in our χ^2 search and we let the computer search for the minimal χ^2 sum for a fit to both $d\sigma/d\Omega$ and A_{on}. In our fits we choose $\delta_{10}=0$ for the $^3P_0$ partial wave whereas R_{10} is a free parameter. For all other LJ values both phase and amplitude in Eq. (7) are allowed to vary, to obtain the best fit. When the complex amplitudes for the partial waves $^3P_0$, $^3S_1$, $^3D_1$, etc. are determined by the minimal χ^2 search, we calculate as a test

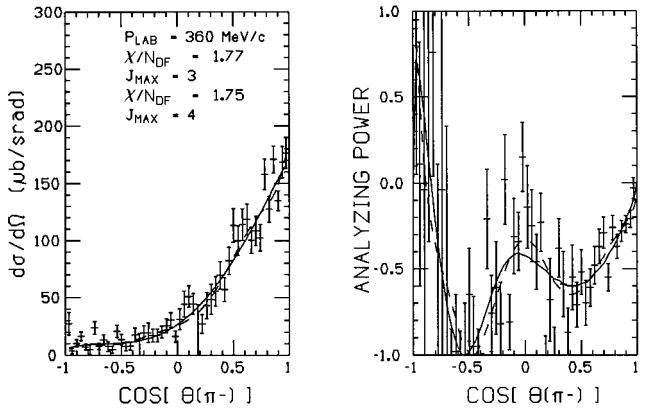

FIG. 1. $d\sigma/d\Omega$ and A_{on} at $p_{\mathrm{lab}}=360$ MeV/c. The solid curves give the fit for $J_{\max}=3$ and the dashed curves are the fit for $J_{\max}=4$.

the total reaction cross section with these amplitudes and compare with the magnitude of the angular integrated experimental cross section

$$\sigma=2\pi\int_{-1}^{1}d\sigma/d\Omega\ d\cos\theta. \tag{9}$$

In part because of the incompleteness of the set of measured observables, we do not find a unique solution, i.e., a unique set of partial wave amplitudes in our χ^2 search. The different solutions depend on the input-start values of the amplitude parameters R_{LJ} and δ_{LJ} and on the way the χ^2 search is performed. However, the minimal value of χ^2 found in the various possible fits are the same. If we had available data on the reaction $\overline{pp}\to\pi^0\pi^0$ or on other spin observables it would be possible to restrict the choice among the various amplitude sets with equally good χ^2.

The data for all measured energies starting from $p_{\mathrm{lab}}=360$ MeV/c up to 1 GeV/c can be fitted with partial wave amplitudes with total angular momentum $J\leqslant 3$. Once we have determined the amplitude values in Eq. (7) at one energy, we use these as start values in our χ^2 search at the neighboring energies. We have also fitted the data with a maximal $J=4$ using the same procedure. It appears that

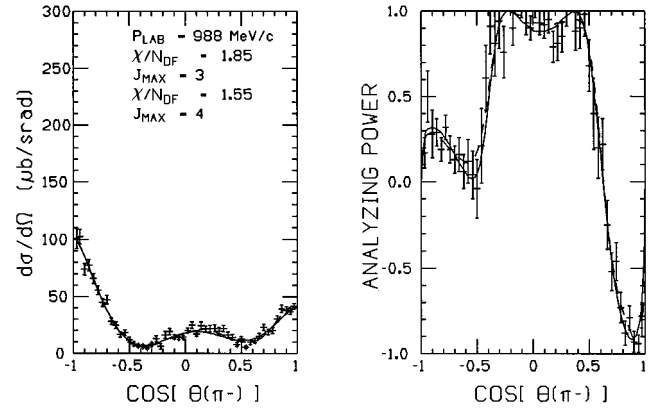

FIG. 2. $d\sigma/d\Omega$ and A_{on} at $p_{\mathrm{lab}}=988$ MeV/c. The solid curves give the fit for $J_{\max}=3$ and the dashed curves are the fit for $J_{\max}=4$.

TABLE I. Examples of χ^2 per degree of freedom at each energy.

$p_{\rm lab}$ (MeV/c)	$\chi^2(J_{\rm max}=2)$	$\chi^2(J_{\rm max}=3)$	$\chi^2(J_{\rm max}=4)$
360	1.96	1.77	1.74
404	1.38	1.12	1.12
467	1.98	1.31	1.18
497	3.04	1.50	1.45
523	2.63	1.45	1.43
585	1.96	1.51	1.57
679	2.17	1.50	1.53
783	2.50	1.49	1.47
886	3.21	1.23	1.13
988	4.39	1.85	1.55

for $\bar{p}$ momenta, $p_{\rm lab}$ above 988 MeV/c, the total χ^2 does become somewhat better when we include the $J=4$ partial wave amplitudes, but below 988 MeV/c the improvement is marginal. As examples, we show two fits in Figs. 1 and 2 for $p_{\rm lab}=360$ and 988 MeV/c. By including the $J=4$ amplitude, we introduce four more parameters, but the χ^2 per degree of freedom hardly improves. It is surprising that so few partial waves with $J_{\rm max}=3$ are sufficient in order to get a satisfactory χ^2 fit to the data.

At the same time we note that both $J=2$ and $J=3$ partial wave amplitudes are essential even at the lowest measured energies because of the shape of the asymmetry A_{on}. The data for A_{on} vs cos θ show two minima even at the lowest energy, $p_{\rm lab}=360$ MeV/c, and a local maximum close to cos $\theta=0$. Previously [13], it has been noted that at least the $J=2$ contribution is needed to reproduce the shape of A_{on}.

In Table I we show the χ^2 per degree of freedom for one set of partial wave amplitude parameters with $J_{\rm max}=3$ as well as the case where $J_{\rm max}=2$ or 4. Listed are the ten momenta between $p_{\rm lab}=360$ and 988 MeV/c, where there are available LEAR data. In Tables II and III we give an example of a set of values for the partial wave amplitudes R_{LJ} and their phases δ_{LJ} found by our χ^2 fit to the data. The normalization of R_{LJ} is such that, if the momentum p in Eqs. (5) and (6) is expressed in GeV/c, the cross section defined in Eq. (1) is in μb/srad. The corresponding χ^2 values are those of Table I for $J_{\rm max}=3$.

TABLE II. Energy dependence of parameters of R_{LJ} and δ_{LJ} for $J_{\rm max}=3$.

$p_{\rm lab}$ (MeV/c)	R_{10}	δ_{10}	R_{01}	δ_{01}	R_{21}	δ_{21}
360	1.60	0	0.50	120	0.80	0
404	1.44	0	0.78	140	0.62	20
467	1.68	0	0.88	115	0.64	30
497	1.60	0	0.74	115	0.70	15
523	1.96	0	0.90	105	0.78	35
585	1.62	0	1.08	125	0.68	75
679	1.42	0	1.22	105	0.88	70
783	1.22	0	1.10	105	1.08	95
886	0.60	0	0.80	95	1.32	100
988	0.14	0	0.48	175	1.50	185

TABLE III. Energy dependence of parameters R_{LJ} and δ_{LJ} for $J_{\rm max}=3$.

$p_{\rm lab}$ (MeV/c)	R_{12}	δ_{12}	R_{32}	δ_{32}	R_{23}	δ_{23}	R_{43}	δ_{43}
360	0.28	35	0.34	-20	0.10	-125	0.06	135
404	0.16	70	0.48	5	0.22	-55	0.08	125
467	0.28	95	0.64	0	0.28	-50	0.20	85
497	0.46	85	0.48	-10	0.32	-110	0.36	100
523	0.34	100	0.38	-25	0.26	-160	0.40	110
585	0.34	135	0.74	0	0.28	-115	0.34	120
679	0.44	100	0.92	-20	0.32	-155	0.42	115
783	0.58	130	1.02	-25	0.52	-165	0.48	125
886	0.56	140	1.14	-15	0.72	-175	0.60	135
988	0.58	225	1.06	60	0.66	-105	0.60	215

In Figs. 3 and 4 we show the energy behavior of our partial wave amplitude parameters, R_{LJ} and δ_{LJ} for all LJ with $J_{\rm max}=3$. The energy dependence indicates a growing importance of $J=2$ and 3 with increasing energy for all solutions. With respect to the $J=0$ and 1 amplitudes, we note that the $^3D_1$ remains important through the entire energy range while the $^3P_0$ and $^3S_1$ amplitudes diminish in importance with increasing energy for one set of solutions. An interesting observation is that for a given J the $L=J+1$ contribution is at least as important as the $L=J-1$ contribution. As discussed above, the $J=2$ and to a lesser extent $J=3$ amplitudes already play significant roles at the lowest momentum 360 MeV/c. The energy dependence of the phases is rather smooth. The sudden increase of all phases between the two highest momenta, 886 and 988 MeV/c for one of our solutions, Tables II and III, is not significant. The reasons being that based on our χ^2 the analysis at 988 MeV/c might need $J=4$ partial waves, and second that the $^3P_0$ amplitude, which is used as our phase reference, has a rather small contribution for this particular set of solutions. Because of the ambiguities present in this analysis, we emphasize that the set of parameters discussed here, and shown in Tables II and III, is one of many possible solutions that give a good fit to the data.

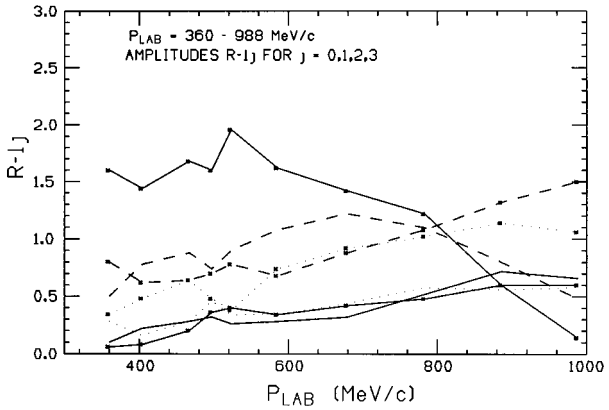

FIG. 3. The amplitudes R_{LJ} of our fit ($J_{\rm max}=3$) vs $p_{\rm lab}$. The curves are only meant to guide the eye. The upper solid curve is $J=0$, dashed curves are $J=1$, dotted curves are $J=2$, lower solid curves are $J=3$. For each J the curve with stars is the $L=J+1$, the curve without stars is $L=J-1$.

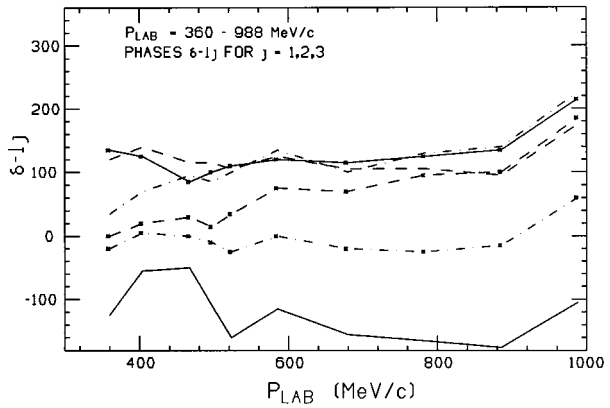

FIG. 4. The phases δ_{LJ} of the amplitudes of our fit ($J_{\max}=3$) vs $p_{\rm lab}$. The curves are labeled as in Fig. 3.

To indicate the level of the ambiguities in our analysis, we give in Tables IV and V a different set of amplitude parameters. This parameter set is a whole new family of amplitudes and these amplitudes have their own energy behavior. It is remarkable that at all energies the corresponding values for the χ^2 are practically identical to the χ^2 tabulated in Table I. This example bears out the ambiguity of the present analysis, and illustrates our point that all local χ^2 minima of our different searches lead to equally good fits to the data. *Only new data at the same energies of other spin observables such as, for example, A_{ss} or A_{ls}, can constrain these ambiguities for the $\overline{p}p\to\pi^-\pi^+$ amplitudes.* Other analyses have used data of the reaction $\overline{p}p\to\pi^0\pi^0$, which unfortunately will only put constraints on the even J ($I=0$) amplitudes.

In Fig. 5 we show the total cross section for this reaction as a function of $p_{\rm lab}$ when we use the amplitudes found in the χ^2 search. For both the parameter sets of Tables II and III, and the alternative set of Tables IV and V, the total cross section for $\overline{p}p\to\pi^-\pi^+$ as a function of $p_{\rm lab}$ agrees with the total cross section of Hasan *et al.* [1] within a few percent. The momentum or energy dependence of each individual J-value contribution to the total cross section is shown in Fig. 5 for the solution corresponding to Tables II and III. The alternative parameter set gives, as expected, a different distribution of individual J-value contributions but leads to the same total cross section. For both parameter sets there is a considerable contribution from $J=2$ at the lowest momentum, $p_{\rm lab}=360$ MeV/c. The $J=3$ contribution to the total cross section is small at 360 MeV/c, but becomes substantial at 500 MeV/c.

TABLE IV. Energy dependence of alternative parameter set of R_{LJ} and δ_{LJ}.

$p_{\rm lab}$ (MeV/c)	R_{10}	δ_{10}	R_{01}	δ_{01}	R_{21}	δ_{21}
360	1.38	0	0.92	150	0.44	-30
404	1.12	0	0.94	140	0.46	-10
467	1.16	0	1.06	115	0.34	-35
497	0.82	0	0.96	115	0.52	-40
523	0.82	0	1.24	115	0.64	-50
585	0.84	0	1.26	150	0.60	-70
679	0.74	0	1.30	160	0.72	-65
783	0.66	0	1.22	220	1.34	-5
886	1.42	0	0.82	235	1.18	35
988	1.24	0	0.66	230	1.04	40

TABLE V. Energy dependence of alternative parameter set R_{LJ} and δ_{LJ}.

$p_{\rm lab}$ (MeV/c)	R_{12}	δ_{12}	R_{32}	δ_{32}	R_{23}	δ_{23}	R_{43}	δ_{43}
360	0.42	90	0.14	-105	0.14	100	0.14	-210
404	0.52	105	0.28	-40	0.06	0	0.24	-180
467	0.76	95	0.42	-25	0.20	25	0.28	-195
497	0.74	100	0.44	-10	0.36	0	0.28	-160
523	0.54	80	0.52	5	0.42	-10	0.26	-115
585	0.64	115	0.68	45	0.32	30	0.30	-90
679	0.70	120	0.92	65	0.40	25	0.36	-60
783	0.50	180	0.88	145	0.46	80	0.56	20
886	0.54	225	0.92	215	0.50	120	0.94	75
988	0.38	225	0.92	240	0.46	130	1.06	95

Finally, in Fig. 6 we show examples of Argand plots for the amplitudes ${}^3P_2,{}^3F_2,{}^3D_3,{}^3G_3$. The amplitudes in this figure are taken from Tables II and III. One should bear in mind that the largest J value equals 3 in the fit producing these amplitudes. In addition, we are considering a very limited energy range. Therefore, we cannot draw any firm conclusion about evidence for resonances in any of these sets of amplitudes. However, from this amplitude analysis it should be clear that at each energy, the $J=2$ and $J=3$ amplitudes play very significant roles, even at the lowest energies. The physics of this annihilation process is largely unknown. It should be noted that annihilation models tend to give a rather small $J=2$ and $J=3$ contributions at these low energies. Until a better theoretical understanding of this very short range reaction is reached, theoretical input in an analysis of these very good data from LEAR is questionable. Figure 6 in particular, invites the question how accurate the parameters in our analysis are. Since we do a separate analysis at each energy and use no mechanism to smooth the result from one energy to the next, the error bars may be substantial. Our

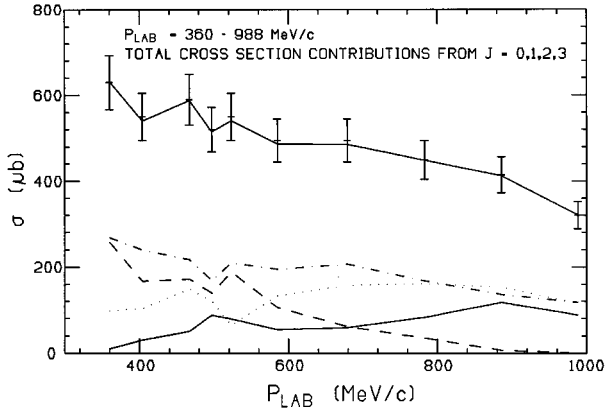

FIG. 5. The total cross section (upper solid curve) for $\overline{p}p\to\pi^-\pi^+$ as a function of $p_{\rm lab}$ for the solutions from Table II and III Data points are from Ref. [1]. Contributions from $J=0,1,2,3$ are shown as, respectively, dashed, dot-dashed, dotted, and solid curves. Again the curves are only meant to guide the eye.

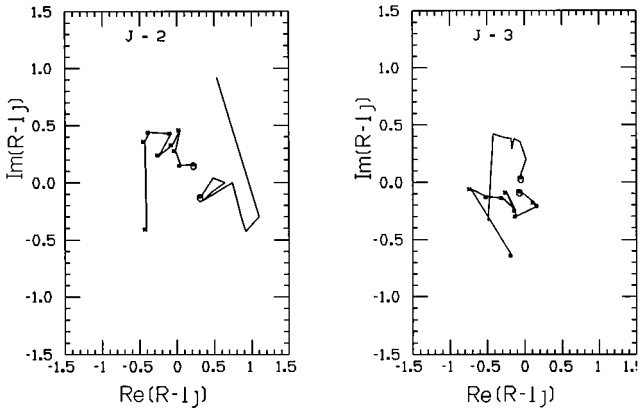

FIG. 6. Argand diagrams for the partial wave amplitudes $3P2$ (solid with stars), $3F2$ (solid), $3D3$ (solid with stars), $3G3$ (solid). These amplitudes are taken from a χ^2 fit with $J_{\max} = 3$, described in Tables II and III. The open circles indicate the lowest energy in all the plots.

simple analysis of the data does not warrant a serious error analysis at this point.

III. DISCUSSION OF RESULTS

It is clear from all our fits that at all momenta below 1 GeV/c, very few partial waves suffice to fit the data. Partial wave amplitudes with $J = 0,1,2$, and 3 are adequate in all cases. Adding the $J = 4$ partial wave amplitude does not improve the χ^2 per degree of freedom in our analysis, except for momenta close to 1 GeV/c. This statement can be made, while no theoretical bias as to the energy- and analytical-behavior of the amplitudes has been imposed on our fits. These results are not inconsistent with the simple model analysis at the higher energies [12]. This earlier work [12] used a diffractive scattering model from a simple black or grey sphere which could explain most of the features of the higher energy data ($p_{\rm lab}$ above 1.5 GeV/c, and above 1.0 GeV/c for $pp \to K^- K^+$). In that model description of the data, the spin-dependent forces were assumed to act in the surface region only. The idea was that since the central region was ''black,'' no detailed information would escape from the central interaction region. Only the more transparent surface region would provide the spin forces giving the asymmetries of this annihilation reaction. No apparent resonances were needed in that simple model description.

In our analysis the data for A_{on} with an apparent local maximum close to $\cos\theta = 0$, and the presence of two minima even at the three lowest energies, requires the presence of the $J = 2$ and $J = 3$ amplitudes. The minimal χ^2 value with $J_{\max} = 2$ is much larger than that for any of the $J_{\max} = 3$ searches. Therefore, we conclude that both the $J = 2$ and $J = 3$ amplitudes are necessary. As mentioned before, adding $J = 4$ does not improve the χ^2 per degree of freedom.

For A_{on} the experimental errors are very large at backward angles for the lowest energies and this prevents us from distinguishing between the solutions that include the $J = 4$ amplitudes from those that only include the $J \leqslant 3$ amplitudes. Note that at the lowest energies, the $J = 4$ amplitudes tend to reduce the backward local maximum of A_{on} compared to the $J_{\max} = 3$ analysis as indicated in Figs. 1 and 2. More accurate data are needed to settle the issue of the necessity of $J = 4$ amplitudes at these energies. From a pure χ^2 point of view the $J = 4$ amplitudes are not really needed for energies below 900 MeV/c.

The observed forward peaking in $d\sigma/d\Omega$ at 360 MeV/c occurs because of a strong cancellation between the even and odd J amplitudes for backward angles ($\theta \approx 180^0$). At our highest energies a backward peak develops, in part because of a constructive interference for backward scattering angles. One notes that at the two highest energies in this analysis ($p_{\rm lab} = 886$ and 988 MeV/c), the forward peak in $d\sigma/d\Omega$ is much smaller in magnitude than the backward peak.

From the amplitude set of Table II (and Table III), it can be seen that the $^3P_0$ amplitude becomes less important with increasing energy whereas for the alternative amplitude set of Tables IV and V, the $^3P_0$ amplitude stays important. In addition, observe that at the highest energies of this analysis the amplitudes $R_{J+1,J}$ are often larger than the corresponding $R_{J-1,J}$. We looked for indications that the initial NN tensor-coupled partial waves would be tensor eigenstates as proposed by Dover and Richard [14]. This can be checked by looking at the phase correlation of f^J_{J-1} and f^J_{J+1}, Eq. (7). From the Tables II through V we only find a phase difference $|\delta^J_{J-1} - \delta^J_{J+1}|$ of 0° or 180° at very few energies. Therefore, in general, the initial NN states are not pure tensor eigenstates and the f^J_{J-1} and f^J_{J+1} are not correlated in phase. We should mention that adding the two $J = 4$ amplitudes, of course, changes the phases and amplitudes of the lower J amplitudes found by imposing $J_{\max} = 3$ in our χ^2 search. The reason is that the $J = 4$ amplitudes can mimic part of the behavior of the lower partial wave amplitudes.

At $p_{\rm lab} = 783$ MeV/c we tested several aspects of our analysis and also examined the hypothesis of Bowcock and Hodgson [9] that only a few partial waves on the periphery of the interaction region are active, and that the central partial wave amplitudes are very small. For this purpose we have made a χ^2 search excluding the $J = 0$ amplitudes and including the $J = 4$ amplitudes. In essence we use the partial wave amplitudes $J = 1,2,3,4$ in our fit. This part of the analysis, inspired by the Bowcock and Hodgson's conjecture, is summarized in Fig. 7 where fits for the three cases $J = 0,1,2,3$, $J = 0,1,2,3,4$, and $J = 1,2,3,4$ at $p_{\rm lab} = 783$ MeV/c are shown on the same graph. All three cases of J-value combinations have comparable total χ^2 per degree of freedom, which are, respectively, 1.49, 1.47, and 1.50. Of course, the standard case of $J_{\max} = 3$ has the smallest number of parameters because the $J = 0$ amplitude involves only two parameters instead of the usual four for the $J \neq 0$ amplitudes. This phenomenon does not extend to other combinations of J values (e.g., excluding both $J = 0$ and $J = 1$ partial waves), and we find no clear evidence for the hypothesis that only the most peripheral partial waves are active. In fact, with only three partial wave amplitudes nonzero like $J = 1,2,3$ or $J = 2,3,4$, the total χ^2 per degree of freedom is far worse than what is shown in Table I for $J_{\max} = 3$. This peculiar phenomenon holds also at other energies.

IV. CONCLUSION

The fact that very few partial waves are needed in the analysis indicates that this annihilation reaction is a very

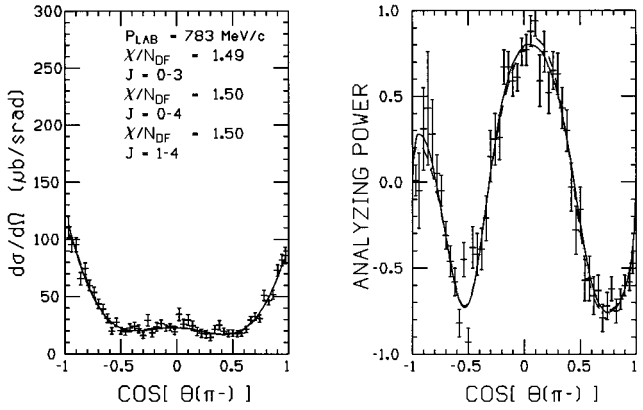

FIG. 7. Fits of $d\sigma/d\Omega$ and A_{on} at 783 MeV/c for various sets of J values as described in the text. Solid curves are for $J=0$–3, dashed curves are for $J=0$–4, and dotted curves are for $J=1$–4. The three curves are almost indistinguishable except for A_{on} at the peak and in the extreme backward direction.

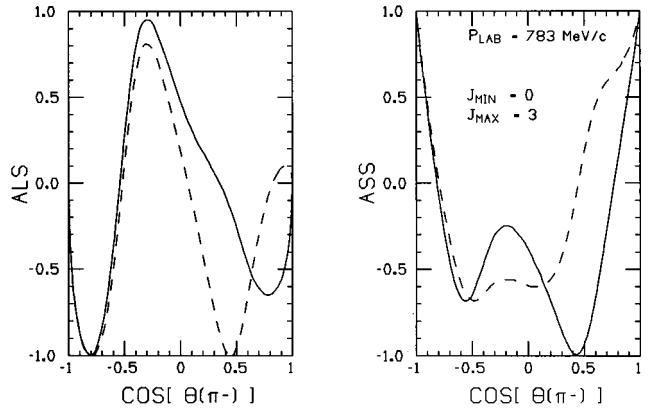

FIG. 8. Predictions for A_{ls} and A_{ss} at 783 MeV/c. Solid line is for regular solution (Tables II + III). Dashed curve is for alternative solution (Tables IV + V).

central process. In contrast, to describe the elastic $\overline{pp}\to\overline{pp}$ scattering at the same energies requires the contributions from partial waves of $J=9$ (and higher) because of the long range pion exchange potential.

As opposed to Oakden and Pennington [10], we find no compelling evidence for resonance behavior of our partial wave amplitudes when plotted in an Argand diagram in the energy range considered, see Figs. 3 and 6. The approach of Oakden and Pennington has some similarities with ours in the sense that none of the methods assumes a specific energy dependence of the amplitudes and both make a sharp truncation of the partial wave series. A different approach is taken by Hasan and Bugg [11] who by starting from a description in terms of a tower of resonances assume a specific energy dependence. A further, unbiased, more refined analysis of these very good data, with the additional constraints of a third measured observable, is needed to settle the question of possible resonance behavior of the amplitudes.

A possible theoretical constraint on the amplitude behavior could come from the analytic continuation of the $\pi N\to\pi N$ scattering amplitudes as is done by Höhler and Pietarinen [15]. So far, this type of analytic continuation from $\pi N\to\pi N$ elastic scattering amplitudes to $\overline{pp}\to\pi^-\pi^+$ amplitudes is very involved and has only been performed for $\overline{pp}$ subthreshold energies [16]. See, however, the analysis of Martin and Oades [8] who did make use of the crossed channel πN elastic scattering data. We believe that further experimental investigation of the reaction $\overline{pp}\to\pi^-\pi^+$ is a more straightforward alternative.

In summary, the present experimental data and several recent analyses of these data for both $\overline{pp}\to\pi^-\pi^+$ and $\overline{pp}\to K^-K^+$ reactions promise a better understanding of these simple, but fundamental annihilation reactions. The analysis described in this paper suggests the following future experiments as necessary in order to clarify the understanding of the $\overline{pp}\to\pi^-\pi^+$ annihilation reaction.

(i) Measurements of this annihilation reaction should be made at antiproton momenta closer to threshold. At very low energies even fewer partial wave amplitudes would contribute and the ambiguities of an analysis would be reduced. However, ambiguities would remain at the energies we considered.

(ii) Data in the exact same momentum range for the reaction $\overline{pp}\to\pi^0\pi^0$, which is described by the isoscalar amplitudes ${}^3P_0, {}^3P_2, {}^3F_2, {}^3F_4, {}^3H_4$, etc., would certainly be extremely useful. However, from the point of view of amplitude analysis, each helicity amplitude would then have to be separated in an isospin I=0 and I=1 part, and only the $J=$even amplitudes are restricted by the $\overline{pp}\to\pi^0\pi^0$ reaction measurements. A measurement of A_{on} for the reaction $\overline{pp}\to\pi^0\pi^0$ would also be very useful and should be possible with the present experimental setup.

(iii) A different and more complete constraint on the analysis of this reaction would come from data on the other spin observables for $\overline{pp}\to\pi^-\pi^+$ with longitudinal and/or transverse polarized beam and target, for example data on A_{ss} or A_{ls}. To illustrate the sensitivity of these two observables, we have given in Fig. 8 the predictions for A_{ls} and A_{ss} for the two parameter sets of Tables II and III and Tables IV and V. As is obvious from the figures the two predictions differ significantly in the forward hemisphere where we believe experiments can be performed more accurately. Some spin transfer observables have been measured for $\overline{pp}$ elastic and charge-exchange scattering at LEAR. No spin-correlation observables have been measured. We propose here the use of polarized antiprotons to obtain data on the observables A_{ls} or A_{ss} for $\overline{pp}\to\pi^-\pi^+$. Such an experiment would settle the debate about the possible resonances inferred from analysis of this reaction.

ACKNOWLEDGMENTS

We thank F. Bradamante for providing us with the LEAR data, and R. Timmermans for many useful discussions on the art of phase shift analyses. We also thank J.-M. Richard for pointing out the relation between the observables, expressed in Eq. (5). This work was supported in part by NSF Grant Nos. PHYS-9310124 and PHYS-9504866.

[1] A. Hasan *et al.*, Nucl. Phys. **B378**, 3 (1992).
[2] E. Eisenhandler *et al.*, Nucl. Phys. **B98**, 109 (1975).
[3] A.A. Carter *et al.*, Phys. Lett. **67B**, 117 (1977).
[4] T. Tanimori *et al.*, Phys. Rev. Lett. **55**, 185 (1985); Phys. Rev. D **41**, 744 (1990).
[5] A.A. Carter, Phys. Lett. **67B**, 122 (1977).
[6] A.D. Martin and M.R. Pennington, Nucl. Phys. **B169**, 216 (1980).
[7] B.R. Martin and D. Morgan, Nucl. Phys. **B176**, 355 (1980).
[8] B.R. Martin and G.C. Oades, Nucl. Phys. **A483**, 669 (1988); see N. Isgur and K. Königsmann, in *Particles and Nuclei*, Proceedings of the Twelfth International Conference, Cambridge, Massachusetts, 1990, edited by J.L. Matthews *et al.*, [Nucl. Phys. **A527**, 491c (1991)].
[9] J.E. Bowcock and D.C. Hodgson, Lett. Nuovo Cimento **28**, 21 (1980).
[10] M.N. Oakden and M.R. Pennington, Nucl. Phys. **A574**, 731 (1994).
[11] A. Hasan and D.V. Bugg, Phys. Lett. B **334**, 215 (1994).
[12] S. Takeuchi, F. Myhrer, and K. Kubodera, in *Proceedings of Intersection between Particle and Nuclear Physics*, AIP Conf. Proc. No. 243 (AIP, New York, 1992) p. 358; Nucl. Phys. **A556**, 601 (1993).
[13] G. Bathas and W.M. Kloet, Phys. Rev. C **47**, 2207 (1993).
[14] C.B. Dover and J.M. Richard, Phys. Rev. C **17**, 1770 (1978).
[15] G. Höhler and E. Pietarinen, Nucl. Phys. **B95**, 210 (1975); G. Höhler, in *Pion–Nucleon Scattering*, edited by K.H. Hellwege, and Landholt-Börnstein (Springer-Verlag, New York, 1983) New Series, Gp I, Vol. 9b, Pt. 2.
[16] G.E. Brown and A. Jackson, *Nucleon-nucleon interaction* (North Holland, Amsterdam, 1976).